

An Axisymmetric Infinite Cylinder with Two Cracks and a Rigid Inclusion

Mete Onur KAMAN and Mehmet Ruşen GEÇİT

*Middle East Technical University, Department of Engineering Sciences, Ankara-TURKEY
e-mail: gecit@metu.edu.tr*

Received 10.08.2006

Abstract

This work considers the analysis of a cracked infinite cylinder with a rigid inclusion. The material of the cylinder is assumed to be linearly elastic and isotropic. The ends of the infinite cylinders are subjected to axial tension. Solution of this problem can be obtained by superposition of solutions for an infinite cylinder subjected to uniformly distributed tensile loads at infinity (I), and an infinite cylinder having a penny-shaped rigid inclusion at $z=0$ and 2 penny-shaped cracks at $z = \pm L$ (II). General expressions for the perturbation problem (II) are obtained by solving Navier equations using Fourier and Hankel transforms. Formulation of the problem is reduced to a system of 3 singular integral equations. By using the Gauss-Lobatto integration formula, these 3 singular integral equations are converted to a system of linear algebraic equations, which are solved numerically.

Key words: Axisymmetric, Infinite cylinder, Penny-shaped crack, Rigid inclusion, Stress intensity factor.

Introduction

Cylinders, like shafts, pins, bolts, screws, pipes, etc., are the most widely used machine elements with axisymmetric geometries, and, due to singularities, they have particular importance in fracture mechanics. They may have discontinuities in the form of holes, notches, cracks, or inclusions, which are very important factors influencing stress distributions in loaded elements. Stresses around these discontinuities may reach very large values in small regions, a phenomenon known as stress concentration. Furthermore, stresses become infinite at the corners of elements or the edges of cracks and inclusions. In such cases, stress concentration cannot be defined as a strength parameter, and it is necessary to consider the stress distributions from a fracture mechanics point of view. Fracture toughness, which is a widely accepted fracture parameter, can be easily calculated in terms of stress intensity factors. For cracked semi-infinite or infinite cylinder configurations subjected to external forces, it is possible to de-

rive closed-form expressions for stresses in the body, assuming isotropic linear elastic material behavior. For linear elastic materials, individual components of stress, strain, and displacement are additive (superposition). In many instances of analytical solutions, the principle of superposition allows stress intensity solutions for complex configurations to be built from simple cases for which the solutions are well established. In this context, the problem of a cracked infinite cylinder with a rigid penny-shaped inclusion has not been solved by the analytical method used in this study.

Sneddon and Welch (1963) analyzed the distribution of the stress in a long circular cylinder of elastic material when it is deformed by the application of pressure to the inner surfaces of a penny-shaped crack situated symmetrically at the center of the cylinder. The equations of the classical theory of elasticity have been reduced to a Fredholm integral equation of the second kind. Benthem and Minderhoud (1972) solved the problem of a solid cylinder compressed axially between rough rigid

stamps. Gupta (1973) considered a semi-infinite cylinder problem with a fixed short end. An exact formulation of the problem in terms of a singular integral equation has been provided. Using transform methods, the axisymmetric end-problem for a semi-infinite elastic circular cylinder has been reduced to a system of singular integral equations by Agarwal (1978). As an application, an axisymmetric solution for joined dissimilar elastic semi-infinite cylinders under uniform tension has been given. Erdol and Erdogan (1978) studied an elastostatic axisymmetric problem for a long thick-walled cylinder containing a ring-shaped internal crack, or an edge crack, using the transform technique. Nied and Erdogan (1983) analyzed a long hollow cylinder containing an axisymmetric circumferential crack subjected to general non-axisymmetric external loads. The problem has been formulated in terms of a system of singular integral equations, with the Fourier coefficients of the derivative of the crack surface displacement as density functions for a cylinder under uniform tension, bending by end couples, or self-equilibrating residual stresses. Isida et al. (1985) made an analysis of an infinite solid containing 2 parallel elliptical cracks located in staggered positions. Xiao et al. (1996) investigated the stress intensity factors of 2 penny-shaped cracks with different sizes in a three-dimensional elastic solid under uniaxial tension. A closed-form analytical solution for the stress intensity factors on the boundaries of the cracks was obtained when the center distance between the 2 cracks is much larger than the cracks. Leung and Su (1998) extended the two-level finite element method (2LFEM) to the accurate analysis of axisymmetric cracks, where both the crack geometry and applied loads were symmetrical about the axis of rotation. Chen (2000) evaluated stress intensity factors in a cylinder with a circumferential crack with an indirect method, the computing compliance method. Lee (2001, 2002) made analyses of the stress distribution in long circular cylinders of elastic material, one containing a penny-shaped crack and the other a circumferential edge crack, when each was subjected to a uniform shearing stress. Meshii and Watanabe (2001) presented the development of a practical method, using prepared tabulated data, to calculate the Mode I stress intensity factor for an inner surface circumferential crack in a finite length cylinder. The method was derived by applying the author's weight function for the crack based on the thin shell theory. Selvadurai (2002) examined the

axial tensile loading of a rigid circular disc, which was bonded to the surface of a half-space weakened by a penny-shaped crack. Tsang et al. (2003) investigated the stress intensity factors of multiple penny-shaped cracks in an elastic solid cylinder under axial tensile loading. The fractal-like finite element method is employed to study the interaction of multiple cracks. An Eigen function expansion method was presented to obtain three-dimensional asymptotic stress fields in the vicinity of the front of a penny-shaped discontinuity, e.g., crack and anticrack (infinitely rigid lamella), subjected to far-field torsion (Mode III), extension/bending (Mode I), and sliding shear/twisting (Mode II) loading (Chaudhuri, 2003).

This study considers the axisymmetric elasticity problem for an infinite cylinder containing 2 concentric penny-shaped cracks at $z = \pm L$ and a penny-shaped rigid inclusion with virtually zero thickness at $z = 0$. The ends of the infinite cylinder of radius A at $z = \pm\infty$ are under the action of axial tensile loads of uniform intensity p_0 . The material of the cylinder is assumed to be linearly elastic and isotropic. The surface of the cylinder is free of stresses. General expressions are obtained by using Hankel and Fourier transforms on Navier equations. First, the boundary conditions at the surface of the infinite cylinder are satisfied. By using the boundary conditions of the cracks and the rigid inclusion, formulation of the problem is reduced to a system of 3 singular integral equations. By using the Gauss-Lobatto integration formula (Krenk, 1978), these singular integral equations are converted to a system of linear algebraic equations, which are solved numerically. Variations in Mode I and Mode II stress intensity factors at the edges of the cracks, and the inclusion, probable propagation angle, and the energy release rate for the cracks are presented in graphical form.

Formulation of the problem

An axisymmetric, linearly elastic, isotropic, and infinite cylinder of radius A , containing 2 concentric penny-shaped cracks of radius a symmetrically located at $z = \pm L$ planes and a concentric penny-shaped rigid inclusion of radius b with negligible thickness at the symmetry plane $z = 0$ is considered. Both ends of this infinite cylinder are subjected to axial tensile loads of uniform intensity p_0 at infinity (Figure 1).

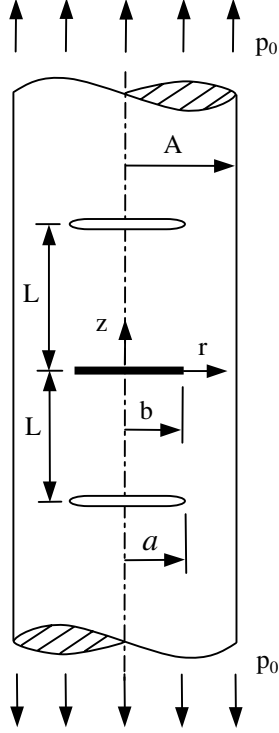


Figure 1. Geometry and loading of the infinite cylinder.

For the linearly elastic, isotropic, and axisymmetric elasticity problems, Navier equations can be written as (Geçit, 1986)

$$(\kappa + 1)\left(\frac{\partial^2 u}{\partial r^2} + \frac{1}{r} \frac{\partial u}{\partial r} - \frac{u}{r^2}\right) + (\kappa - 1)\frac{\partial^2 u}{\partial z^2} + 2\frac{\partial^2 w}{\partial r \partial z} = 0,$$

$$2\left(\frac{\partial^2 u}{\partial r \partial z} + \frac{1}{r} \frac{\partial u}{\partial z}\right) + (\kappa - 1)\left(\frac{\partial^2 w}{\partial r^2} + \frac{1}{r} \frac{\partial w}{\partial r}\right) +$$

$$(\kappa + 1)\frac{\partial^2 w}{\partial z^2} = 0, \quad (1a,b)$$

where u and w are displacements in r - and z -directions in the cylindrical coordinate system $\kappa = 3 - 4\nu$, and ν is the Poisson's ratio. Necessary stress-displacement relations can be listed as follows (Geçit, 1986):

$$\sigma_r = \frac{\mu}{\kappa - 1} \left[(\kappa + 1) \frac{\partial u}{\partial r} + (3 - \kappa) \left(\frac{u}{r} + \frac{\partial w}{\partial z} \right) \right],$$

$$\sigma_z = \frac{\mu}{\kappa - 1} \left[(\kappa + 1) \frac{\partial w}{\partial z} + (3 - \kappa) \left(\frac{\partial u}{\partial r} + \frac{u}{r} \right) \right],$$

$$\tau_{rz} = \mu \left(\frac{\partial u}{\partial z} + \frac{\partial w}{\partial r} \right), \quad (2a-c)$$

where σ and τ denote normal and shearing stresses, and μ is the shear modulus. Solution for the infinite cylinder having a rigid penny-shaped inclusion and 2 penny-shaped cracks, which is loaded at infinity, is obtained by superposition of the following 2 problems: (I) an infinite cylinder subjected to uniformly distributed axial tension of intensity p_0 at infinity, with no cracks or inclusion; (II) an infinite cylinder with an inclusion and 2 cracks for which the loading is the negative of the stresses at the location of the cracks and displacements at the location of the inclusion calculated from the solution of problem (I). General expressions of the displacement and the stress components for the perturbation problem with no loads at infinity can be obtained by adding the general expressions of (II-i) an infinite cylinder containing 2 penny-shaped cracks of radius a symmetrically located at $z = \pm L$ planes, (II-ii) an infinite cylinder having a penny-shaped rigid inclusion of radius b at the symmetry plane $z = 0$, and (II-iii) an infinite cylinder without cracks and inclusion under the action of arbitrary axisymmetric loading (Figure 2). This is necessary in order for the expressions to contain a sufficient number of unknowns so that all of the boundary conditions can be satisfied.

General expressions for the infinite cylinder ($0 \leq r < A$) problems may be adequately obtained from infinite medium ($0 \leq r < \infty$) solutions with appropriate boundary conditions imposed at $r = A$. Due to symmetry about the $z = 0$ plane, it is sufficient to solve the problem only in the upper half space $z \geq 0$. By these considerations, general expressions for the sub-problems can be obtained from the solution of Eqs. (1) and (2), which can be written in the form

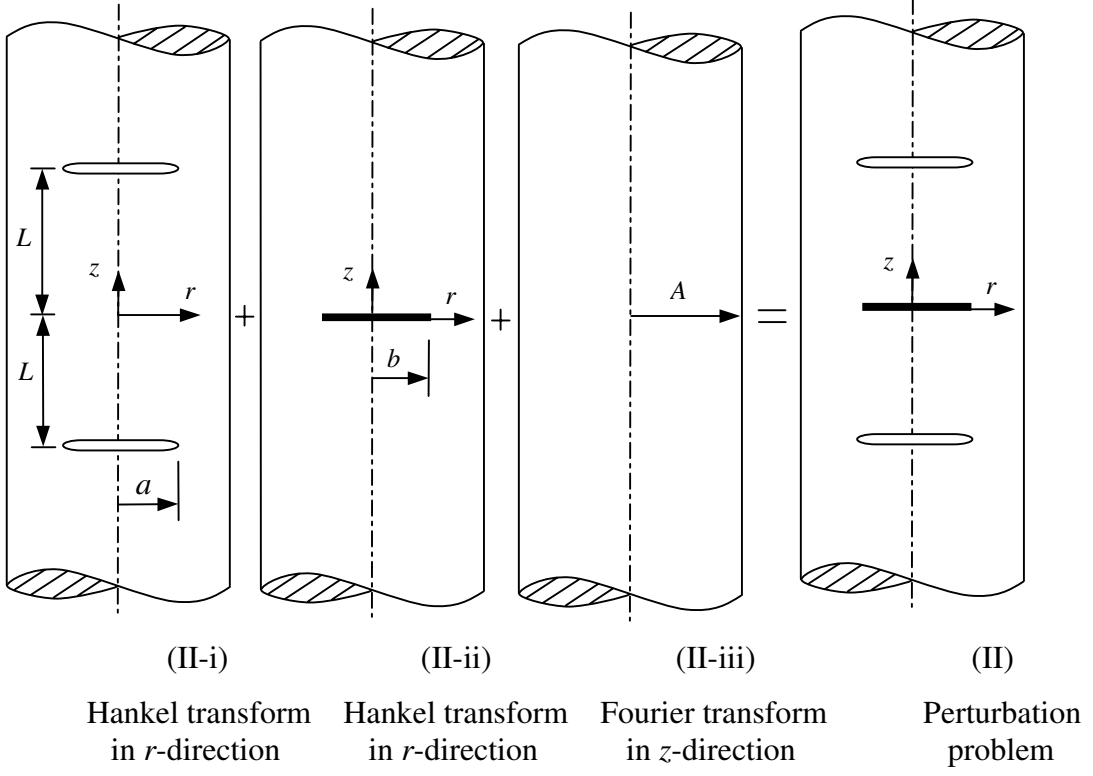


Figure 2. Addition of several solutions for the perturbation problem.

$$\begin{aligned}
 u_i(r, z) &= \frac{1}{2(\kappa+1)} \int_0^\infty \{[(\kappa-1-2\alpha L-2\alpha z)F_1(\alpha) + (1+\kappa-2\alpha L-2z\alpha)F_2(\alpha)] e^{-\alpha(L+z)} \\
 &\quad + [(\kappa-1-2\alpha L+2\alpha z)F_1(\alpha) - (1+\kappa-2\alpha L+2\alpha z)F_2(\alpha)] e^{-\alpha(L-z)}\} J_1(\alpha r) d\alpha, \\
 w_i(r, z) &= \frac{-1}{2(\kappa+1)} \int_0^\infty \{[(1+\kappa+2\alpha L+2\alpha z)F_1(\alpha) + (1-\kappa-2\alpha L-2\alpha z)F_2(\alpha)] e^{-\alpha(L+z)} \\
 &\quad - [(1+\kappa+2\alpha L-2\alpha z)F_1(\alpha) + (1-\kappa-2\alpha L+2\alpha z)F_2(\alpha)] e^{-\alpha(L-z)}\} J_0(\alpha r) d\alpha, \\
 \sigma_{ri}(r, z) &= \frac{2\mu}{\kappa+1} \int_0^\infty \{[(1-\alpha L-\alpha z)F_1(\alpha) + (2-\alpha L-\alpha z)F_2(\alpha)] e^{-\alpha(L+z)} \\
 &\quad + [(1-\alpha L+\alpha z)F_1(\alpha) - (2-\alpha L+\alpha z)F_2(\alpha)] e^{-\alpha(L-z)}\} \alpha J_0(\alpha r) d\alpha \\
 &\quad + \frac{\mu}{\kappa+1} \int_0^\infty \{[(1-\kappa+2\alpha L+2\alpha z)F_1(\alpha) + (1+\kappa-2\alpha L-2\alpha z)F_2(\alpha)] e^{-\alpha(L+z)}
 \end{aligned} \tag{3a,b}$$

$$\begin{aligned}
 & + [(1 - \kappa + 2\alpha L - 2\alpha z)F_1(\alpha) + (1 + \kappa - 2\alpha L + 2\alpha z)F_2(\alpha)] e^{-\alpha(L-z)} \left\} \frac{J_1(\alpha r)}{r} d\alpha, \\
 \sigma_{zi}(r, z) & = \frac{2\mu}{\kappa + 1} \int_0^\infty \{[(1 + \alpha L + \alpha z)F_1(\alpha) - \alpha(L + z)F_2(\alpha)] e^{-\alpha(L+z)} \\
 & + [(1 + \alpha L - \alpha z)F_1(\alpha) - \alpha(L - z)F_2(\alpha)] e^{-\alpha(L-z)}\} \alpha J_0(\alpha r) d\alpha, \\
 \tau_{rzi}(r, z) & = \frac{2\mu}{\kappa + 1} \int_0^\infty \{[\alpha(L + z)F_1(\alpha) + (1 - \alpha L - \alpha z)F_2(\alpha)] e^{-\alpha(L+z)} \\
 & + [-\alpha(L + z)F_1(\alpha) - (1 - \alpha L + \alpha z)F_2(\alpha)] e^{-\alpha(L-z)}\} \alpha J_1(\alpha r) d\alpha, \tag{4a-c}
 \end{aligned}$$

where J_0 and J_1 are the Bessel functions of the first kind of order zero and one, respectively,

$$F_1(\alpha) = \int_0^\infty f_1(r)rJ_1(\alpha r)dr, \quad F_2(\alpha) = \int_0^\infty f_2(r)rJ_0(\alpha r)dr, \tag{5a,b}$$

$$\frac{\partial}{\partial r} [w_{i-2}(r, L^+)] - \frac{\partial}{\partial r} [w_{i-1}(r, L^-)] = f_1(r), \quad (0 \leq r < \infty)$$

$$\frac{1}{r} \frac{\partial}{\partial r} [ru_{i-2}(r, L^+)] - \frac{1}{r} \frac{\partial}{\partial r} [ru_{i-1}(r, L^-)] = f_2(r), \quad (0 \leq r < \infty) \tag{6a,b}$$

such that $f_i(r) = 0$, ($i = 1, 2$) when ($a < r < \infty$), in ($0 \leq z \leq L$) for II-i,

$$\begin{aligned}
 u_{ii}(r, z) & = \frac{1}{2\mu(\kappa + 1)} \int_0^\infty (-\kappa + \alpha z)F_3(\alpha) e^{-\alpha z} J_1(\alpha r) d\alpha, \\
 w_{ii}(r, z) & = \frac{1}{2\mu(\kappa + 1)} \int_0^\infty \alpha z F_3(\alpha) e^{-\alpha z} J_0(\alpha r) d\alpha, \tag{7a,b}
 \end{aligned}$$

$$\sigma_{rii}(r, z) = \frac{1}{\kappa + 1} \int_0^\infty (\kappa - \alpha z) F_3(\alpha) e^{-\alpha z} [J_1(\alpha r)/r] d\alpha$$

$$-\frac{1}{2(\kappa + 1)} \int_0^\infty (3 + \kappa - 2\alpha z)F_3(\alpha) e^{-\alpha z} \alpha J_0(\alpha r) d\alpha,$$

$$\sigma_{zii}(r, z) = \frac{1}{2(\kappa + 1)} \int_0^\infty (\kappa - 1 - 2\alpha z)F_3(\alpha) e^{-\alpha z} \alpha J_0(\alpha r) d\alpha,$$

$$\tau_{rz\ ii}(r, z) = \frac{1}{2(\kappa + 1)} \int_0^{\infty} (1 + \kappa - 2\alpha z) F_3(\alpha) e^{-\alpha z} \alpha J_1(\alpha r) d\alpha, \quad (8a-c)$$

where

$$F_3(\alpha) = \int_0^{\infty} f_3(r) r J_1(\alpha r) dr, \quad (9)$$

$$\tau_{rz\ ii}(r, 0^+) - \tau_{rz\ ii}(r, 0^-) = f_3(r), \quad (0 \leq r < \infty) \quad (10)$$

$f_3(r)$ is the jump in the shearing stress τ_{rz} through the rigid inclusion and it is such that $f_3(r) = 0$ when ($b < r < \infty$), in ($0 \leq z < \infty$) for II-ii, and

$$u_{iii}(r, z) = \frac{1}{\pi} \int_0^{\infty} [-c_1 I_1(\alpha r) + 2c_2 \alpha r I_0(\alpha r)] \cos(\alpha z) d\alpha,$$

$$w_{iii}(r, z) = \frac{1}{\pi} \int_0^{\infty} \{c_1 I_0(\alpha r) - 2c_2 [(\kappa + 1) I_0(\alpha r) + \alpha r I_1(\alpha r)]\} \sin(\alpha z) dz, \quad (11a, b)$$

$$\sigma_{r\ iii}(r, z) = \frac{2\mu}{\pi} \int_0^{\infty} \{c_1 [I_1(\alpha r)/r - \alpha I_0(\alpha r)] + c_2 [(\kappa - 1)\alpha I_0(\alpha r) + 2\alpha^2 r I_1(\alpha r)]\} \cos(\alpha z) d\alpha,$$

$$\sigma_{z\ iii}(r, z) = \frac{2\mu}{\pi} \int_0^{\infty} \{c_1 \alpha I_0(\alpha r) - c_2 [(\kappa + 5)\alpha I_0(\alpha r) + 2\alpha^2 r I_1(\alpha r)]\} \cos(\alpha z) d\alpha,$$

$$\tau_{rz\ iii}(r, z) = \frac{2\mu}{\pi} \int_0^{\infty} \{c_1 \alpha I_1(\alpha r) - c_2 [(\kappa + 1)\alpha I_1(\alpha r) + 2\alpha^2 r I_0(\alpha r)]\} \sin(\alpha z) d\alpha, \quad (12a-c)$$

where I_0 and I_1 are the modified Bessel functions of the first kind of order zero and one, respectively, and c_1 and c_2 are arbitrary constants in ($0 \leq z < \infty$) for II-iii.

Now, the general expressions for the infinite medium containing 2 penny-shaped cracks and a penny-shaped inclusion that is subjected to arbitrary axisymmetric loads (not at infinity) may be obtained when the individual expressions are added:

$$u_{II} = u_i + u_{ii} + u_{iii},$$

$$w_{II} = w_i + w_{ii} + w_{iii}, \quad (13a, b)$$

$$\sigma_{rII} = \sigma_{ri} + \sigma_{rii} + \sigma_{riii},$$

$$\sigma_{zII} = \sigma_{zi} + \sigma_{zii} + \sigma_{ziii},$$

$$\tau_{rzII} = \tau_{rzi} + \tau_{rzil} + \tau_{rziil}. \quad (14a-c)$$

These expressions may give those for the perturbation problem for an infinite cylinder with a stress-free surface if they are forced to satisfy the homogeneous boundary conditions

$$\begin{aligned} \sigma_{rII}(A, z) &= 0, \quad (0 \leq z < \infty) \\ \tau_{rzII}(A, z) &= 0, \quad (0 \leq z < \infty) \end{aligned} \quad (15a,b)$$

which give

$$\begin{aligned} c_1 &= A\alpha \{[(\kappa - 1)I_0(\alpha A) + 2A\alpha I_1(\alpha A)]\alpha E_1 + [(\kappa + 1)I_1(\alpha A) + 2A\alpha I_0(\alpha A)]E_2\} / d_0, \\ c_2 &= -\{[A\alpha I_0(\alpha A) - I_1(\alpha A)]\alpha E_1 + A\alpha I_1(\alpha A)E_2\} / d_0, \end{aligned} \quad (16a,b)$$

in which one may show that

$$\begin{aligned} E_1 &= 4 \int_0^a [d_1 \cos(\alpha L)f_1(t) + d_2 \sin(\alpha L)f_2(t)] t dt - (1/\mu) \int_0^b d_3 f_3(t) t dt, \\ E_2 &= 4 \int_0^a \{d_4 \cos(\alpha L)f_1(t) + [d_5 \alpha + d_6/A - (\kappa + 1)/2\alpha^2 A^2] \sin(\alpha L)f_2(t)\} t dt \\ &\quad - (1/\mu) \int_0^b \{d_4 + (\kappa + 1) [K_0(\alpha A) + K_1(\alpha A)/\alpha A] I_1(\alpha t)/2\} f_3(t) t dt, \end{aligned} \quad (17a,b)$$

$$d_0 = (\kappa + 1) [2 A^2 \alpha^2 I_0^2(A\alpha) - (1 + \kappa + 2A^2 \alpha^2) I_1^2(A\alpha)],$$

$$d_1 = AK_0(\alpha A)I_1(\alpha t) - tK_1(\alpha A)I_0(\alpha t),$$

$$d_2 = AK_0(\alpha A)I_0(\alpha t) - tK_1(\alpha A)I_1(\alpha t),$$

$$d_3 = d_1 + (\kappa + 1)K_1(\alpha A)I_1(\alpha t)/2\alpha,$$

$$d_4 = \alpha AK_1(\alpha A)I_1(\alpha t) - \alpha tK_0(\alpha A)I_0(\alpha t) + d_3/A,$$

$$d_5 = AK_1(\alpha A)I_0(\alpha t) - tK_0(\alpha A)I_1(\alpha t),$$

$$d_6 = d_2 + (\kappa + 1)K_1(\alpha A)I_0(\alpha t)/2\alpha, \quad (18a-g)$$

K_0 and K_1 are the modified Bessel functions of the second kind of order zero and one, respectively. Then, with the addition of the uniform solution (Artem and Geçit, 2002; Kaman, 2006; Toygar and Geçit, 2006), general expressions for the problem of an infinite cylinder with 2 cracks ($0 \leq r < a$, $z = \pm L$), an inclusion

($0 \leq r < b$, $z = 0$), and a stress-free lateral surface ($r = A$) that is subjected to uniaxial tension of intensity p_0 at $z = \pm \infty$ become

$$\begin{aligned}
 u_{cyl}(r, z) &= \frac{3 - \kappa}{\kappa - 7} \frac{p_0}{2\mu} r + \frac{1}{\kappa + 1} \int_0^a [d_{11}(r, z, t)f_1(t) + d_{12}(r, z, t)f_2(t)] t dt \\
 &\quad + \frac{1}{\mu(\kappa + 1)} \int_0^b d_{13}(r, z, t)f_3(t) t dt, \\
 w_{cyl}(r, z) &= -\frac{4}{\kappa - 7} \frac{p_0}{2\mu} z + \frac{1}{\kappa + 1} \int_0^a [d_{21}(r, z, t)f_1(t) + d_{22}(r, z, t)f_2(t)] t dt \\
 &\quad + \frac{1}{\mu(\kappa + 1)} \int_0^b d_{23}(r, z, t)f_3(t) t dt, \tag{19a,b}
 \end{aligned}$$

$$\begin{aligned}
 \sigma_{rcyl}(r, z) &= \frac{\mu}{\kappa + 1} \int_0^a [d_{31}(r, z, t)f_1(t) + d_{32}(r, z, t)f_2(t)] t dt \\
 &\quad + \frac{1}{\kappa + 1} \int_0^b d_{33}(r, z, t)f_3(t) t dt,
 \end{aligned}$$

$$\begin{aligned}
 \sigma_{zcyl}(r, z) &= p_0 + \frac{\mu}{\kappa + 1} \int_0^a [d_{41}(r, z, t)f_1(t) + d_{42}(r, z, t)f_2(t)] t dt \\
 &\quad + \frac{1}{\kappa + 1} \int_0^b d_{43}(r, z, t)f_3(t) t dt,
 \end{aligned}$$

$$\tau_{rcyl}(r, z) = \frac{\mu}{\kappa + 1} \int_0^a [d_{51}(r, z, t)f_1(t) + d_{52}(r, z, t)f_2(t)] t dt + \frac{1}{\kappa + 1} \int_0^b d_{53}(r, z, t)f_3(t) t dt, \tag{20a-c}$$

where $d_{ij}(r, z, t)$, ($i = 1 - 5$, $j = 1 - 3$) have long expressions in the form of infinite integrals containing Bessel functions, etc. and are given in Kaman (2006).

Integral equations

The expressions for the stresses and the displacements, Eqs. (19) and (20), contain 3 unknown functions, $f_i(t)$, ($i = 1 - 3$). Since crack surfaces are free of stress and the rigid inclusion is assumed to be perfectly bonded to the cylinder, the stress and the displacement expressions must satisfy the following conditions

$$\sigma_z(r, L) = 0, \quad (0 \leq r < a)$$

$$\tau_{rz}(r, L) = 0, \quad (0 \leq r < a) \quad (21a,b)$$

on the crack and

$$u(r, 0) = 0, \quad (0 \leq r < b) \quad (21c)$$

on the rigid inclusion. Eqs. (21a) and (21b) are stress type boundary conditions, while Eq. (21c) is a displacement type, which is satisfied if

$$\frac{1}{r} \frac{\partial}{\partial r} [ru(r, 0)] = 0 \quad (0 \leq r < b) \quad (21d)$$

is satisfied instead. Now, Eqs. (21a), (21b), and (21d) all are of the same (stress) type conditions.

Substituting Eqs. (19) and (20) in Eqs. (21a), (21b), and (21d), and noting that $f_1(t)$ and $f_3(t)$ are odd, and $f_2(t)$ is even, the following singular integral equations may be obtained

$$\begin{aligned} & \int_{-a}^a \{f_1(t) [1/(t-r) + M_2(r, t) + |t| N_{11}(r, t) + |t| S_1(r, t)] + f_2(t) [N_{12}(r, t) + S_2(r, t)] |t|\} dt \\ & + (1/2\mu) \int_{-b}^b f_3(t) [N_{13}(r, t) + S_3(r, t)] |t| dt = -(\kappa + 1)\pi p_0 / 2\mu, \quad (-a < r < a) \\ & \int_{-a}^a \{f_1(t) [N_{21}(r, t) + S_4(r, t)] |t| + f_2(t) [1/(t-r) + M_1(r, t) + |t| N_{22}(r, t) + |t| S_5(r, t)]\} dt \\ & + (1/8\mu) \int_{-b}^b f_3(t) [2N_{23}(r, t) + S_6(r, t)] |t| dt = 0, \quad (-a < r < a) \\ & \int_{-a}^a \{f_1(t) [N_{31}(r, t) + S_7(r, t)] + f_2(t) [N_{32}(r, t) + S_8(r, t)]\} |t| dt \\ & + (1/2\mu) \int_{-b}^b f_3(t) [-\kappa/(t-r) - \kappa M_2(r, t) + |t| N_{33}(r, t)] dt \\ & = (\kappa - 3)(\kappa + 1)\pi p_0 / 2\mu(\kappa - 7), \quad (-b < r < b) \end{aligned} \quad (22a-c)$$

where

$$M_i(r, t) = [m_i(r, t) - 1] / (t - r), \quad (i = 1, 2), \quad (23a,b)$$

$$m_1(r, t) = \begin{cases} |t/r| E(|t/r|), & |t| < |r| \\ E(|r/t|)t^2/r^2 - K(|r/t|)(t^2 - r^2)/r^2, & |t| > |r| \end{cases},$$

$$m_2(r, t) = \begin{cases} |r/t| E(|t/r|) + K(|t/r|)(t^2 - r^2)/|tr| & |t| < |r| \\ E(|r/t|), & |t| > |r| \end{cases} \quad (24a,b)$$

in which K and E are the complete elliptic integrals of the first and the second kinds, respectively. The kernels $N_{ij}(r, t)$ ($i, j = 1 - 3$) are in the form of improper integrals,

$$N_{ij}(r, t) = \int_0^{\infty} K_{ij}(r, t, \alpha) d\alpha, \quad (i, j = 1 - 3) \quad (25)$$

where the integrands $K_{ij}(r, t, \alpha)$, ($i, j = 1 - 3$) together with $S_i(r, t)$, ($i = 1 - 8$) containing complete elliptic integrals are given in the Appendix. The 3 singular integral equations, Eqs. (22a), (22b), and (22c) must be solved in such a way that the single-valuedness conditions for the cracks and the equilibrium equation for the rigid inclusion

$$\int_{-a}^a f_i(t) t dt = 0, \quad (i = 1, 2), \quad \int_{-b}^b f_3(t) t dt = 0 \quad (26a-c)$$

are also satisfied. In Eqs. (22a), (22b), and (22c), the simple Cauchy kernel, $1/(t - r)$, becomes unbounded when $t = r$. The unknown functions, $f_i(t)$, ($i = 1 - 3$), are expected to have integrable singularities at the respective edges of cracks and the inclusion. The singular behavior of these unknown functions can be determined by writing

$$f_i(t) = f_i^*(t) (a^2 - t^2)^{-\beta}, \quad (i = 1, 2), \quad (0 < Re(\beta) < 1)$$

$$f_3(t) = f_3^*(t) (b^2 - t^2)^{-\gamma}, \quad (0 < Re(\gamma) < 1) \quad (27a-c)$$

where $f_i^*(t)$, ($i = 1 - 3$), are Hölder-continuous functions (Muskhelishvili, 1953) in the respective intervals $(-a, a)$ and $(-b, b)$. β and γ are unknown constants, which can be calculated by examining the

$$r = a\psi, \quad t = a\phi, \quad (-a < (r, t) < a, \quad -1 < (\psi, \phi) < 1) \quad (29a,b)$$

and η and ε on the inclusion by

$$r = b\varepsilon, \quad t = b\eta, \quad (-b < (r, t) < b, \quad -1 < (\varepsilon, \eta) < 1) \quad (30a,b)$$

the system of singular integral equations, Eqs. (22) and (26), take the following form

$$\int_{-1}^1 \left\{ \overline{F}_1(\phi) (1 - \phi^2)^{-1/2} [1/(\phi - \psi) + \overline{M}_2(\psi, \phi) + |\phi| \overline{N}_{11}(\psi, \phi) + |\phi| \overline{S}_1(\psi, \phi)] \right. \\ \left. + \overline{F}_2(\phi) (1 - \phi^2)^{-1/2} [\overline{N}_{12}(\psi, \phi) + \overline{S}_2(\psi, \phi)] |\phi| \right\} d\phi$$

integral equations, Eqs. (22a) and (22b) near the ends $r = \mp a$, and Eq. (22c) near the ends $r = \mp b$. By substituting Eq. (27) in Eqs. (22a), (22b), and (22c), calculating the integrals near $r = \mp a$ and $r = \mp b$ with the help of the complex function technique given in Muskhelishvili (1953), following a procedure similar to that given in Cook and Erdogan (1972), one can obtain the following characteristic equations:

$$\cot(\pi\beta) = 0, \quad (0 \leq Re(\beta) < 1) \quad (a < A) \quad (28a)$$

at the edge $r = a$, $z = L$ of the penny-shaped crack,

$$\cot(\pi\gamma) = 0, \quad (0 \leq Re(\gamma) < 1) \quad (b < A) \quad (28b)$$

at the edge $r = b$, $z = 0$ of the penny-shaped inclusion. The acceptable numerical value for β is $1/2$ from Eq. (28a). This is the very well known result for an embedded crack tip in a homogeneous medium (Cook and Erdogan, 1972; Erdol and Erdogan, 1978; Artem and Geçit, 2002; Toygar and Geçit, 2006). Similarly, Eq. (28b) gives $\gamma = 1/2$, which is in agreement with previous results (Erdogan et al., 197n; Gupta, 1974; Nied and Erdogan, 1983; Artem and Geçit, 2002; Yetmez and Geçit, 2005; Toygar and Geçit, 2006).

Solution of integral equations

The integral equations will be expressed in terms of non-dimensional quantities. Defining non-dimensional variables ϕ and ψ on the crack by

$$- \int_{-1}^1 \overline{\overline{F_3}}(\eta) (1 - \eta^2)^{-1/2} [\overline{N_{13}}(\psi, \eta) + \overline{S_3}(\psi, \eta)] (|\eta|/\kappa) d\eta = \pi(\kappa + 1)/\kappa, \quad (-1 < \psi < 1)$$

$$\int_{-1}^1 \left\{ \overline{\overline{F_1}}(\phi) (1 - \phi^2)^{-1/2} [\overline{N_{21}}(\psi, \phi) + \overline{S_4}(\psi, \phi)] |\phi| \right.$$

$$\left. + \overline{\overline{F_2}}(\phi) (1 - \phi^2)^{-1/2} [1/(\phi - \psi) + \overline{M_1}(\psi, \phi) + |\phi| \overline{N_{22}}(\psi, \phi) + |\phi| \overline{S_5}(\psi, \phi)] \right\} d\phi$$

$$- \int_{-1}^1 \overline{\overline{F_3}}(\eta) (1 - \eta^2)^{-1/2} [\overline{N_{23}}(\psi, \eta) + \overline{S_6}(\psi, \eta)] (|\eta|/\kappa) d\eta = 0, \quad (-1 < \psi < 1)$$

$$\int_{-1}^1 \left\{ \overline{\overline{F_1}}(\phi) (1 - \phi^2)^{-1/2} [\overline{N_{31}}(\varepsilon, \phi) + \overline{S_7}(\varepsilon, \phi)] + \overline{\overline{F_2}}(\phi) (1 - \phi^2)^{-1/2} [\overline{N_{32}}(\varepsilon, \phi) + \overline{S_8}(\varepsilon, \phi)] \right\} |\phi| d\phi$$

$$+ \int_{-1}^1 \overline{\overline{F_3}}(\eta) (1 - \eta^2)^{-1/2} [1/(\eta - \varepsilon) + \overline{M_2}(\varepsilon, \eta) - (|\eta|/\kappa) \overline{N_{33}}(\varepsilon, \eta)] d\eta$$

$$= 2\pi(\kappa - 3)(\kappa + 1)/(7 - \kappa)\kappa, \quad (-1 < \varepsilon < 1) \quad (31a-c)$$

$$\int_{-1}^1 \overline{\overline{F_i}}(\phi) (1 - \phi^2)^{-1/2} \phi d\phi = 0, \quad (i = 1 - 3), \quad (32a-c)$$

where

$$\overline{\overline{F_i}}(\phi) = -2\mu(1 - \phi^2)^{1/2} f_i(a\phi)/\kappa p_0, \quad (i = 1, 2), \quad \overline{\overline{F_3}}(\eta) = (1 - \eta^2)^{1/2} f_3(b\eta)/p_0, \quad (33a-c)$$

$\overline{M_i}$ ($i = 1, 2$), $\overline{N_{ij}}$ ($i, j = 1 - 3$), $\overline{S_i}$ ($i = 1 - 8$) are dimensionless kernels, as defined by Kaman (2006). The integrals in Eqs. (31) and (32) may be calculated by the use of the Gauss-Lobatto integration formula (Krenk, 1978; Artem and Geçit, 2002). Then, Eqs. (31) and (32) may be put into the form

$$\begin{aligned} & \sum_{i=1}^{n/2} C_i \left\{ \overline{\overline{F_1}}(\phi_i) [m_4(\psi_j, \phi_i) + \phi_i \overline{N_{11}}(\psi_j, \phi_i) + \phi_i \overline{S_1}(\psi_j, \phi_i)] \right. \\ & \left. + \overline{\overline{F_2}}(\phi_i) [\overline{N_{12}}(\psi_j, \phi_i) + \overline{S_2}(\psi_j, \phi_i)] \phi_i - \overline{\overline{F_3}}(\eta_i) [\overline{N_{13}}(\psi_j, \eta_i) + \overline{S_3}(\psi_j, \eta_i)] (\eta_i/\kappa) \right\} \\ & = (\kappa + 1)/\kappa, \quad (j = 1, \dots, n/2) \end{aligned}$$

$$\sum_{i=1}^{n/2} C_i \left\{ \overline{\overline{F_1}}(\phi_i) [\overline{N_{21}}(\psi_j, \phi_i) + \overline{S_4}(\psi_j, \phi_i)] \phi_i \right.$$

$$\begin{aligned}
 & + \overline{\overline{F}}_2(\phi_i) [m_3(\psi_j, \phi_i) + \phi_i \overline{\overline{N}}_{22}(\psi_j, \phi_i) + \phi_i \overline{\overline{S}}_5(\psi_j, \phi_i)] \\
 & - \overline{\overline{F}}_3(\eta_i) [\overline{\overline{N}}_{23}(\xi_j, \eta_i) + \overline{\overline{S}}_6(\xi_j, \eta_i)] (\eta_i^2/\kappa) \Big\} = 0, \quad (j = 1, \dots, n/2) \\
 & \sum_{i=1}^{n/2} C_i \left\{ \overline{\overline{F}}_1(\phi_i) [2\overline{\overline{N}}_{31}(\varepsilon_j, \phi_i) + 2\overline{\overline{S}}_7(\varepsilon_j, \phi_i)] \phi_i + \overline{\overline{F}}_2(\phi_i) [2\overline{\overline{N}}_{32}(\varepsilon_j, \phi_i) + 2\overline{\overline{S}}_8(\varepsilon_j, \phi_i)] \phi_i \right. \\
 & \left. + F_3(\eta_i) [m_4(\varepsilon_j, \eta_i) - (2\eta_i/\kappa)\overline{\overline{N}}_{33}(\varepsilon_j, \eta_i)] \right\} = 2(\kappa - 3)(\kappa + 1)/(7 - \kappa)\kappa, \\
 & (j = 1, \dots, n/2) \tag{34a-c}
 \end{aligned}$$

where

$$\begin{aligned}
 m_3(\psi_j, \phi_i) &= \begin{cases} [2\phi_i/(\phi_i^2 - \psi_j^2)] E(\phi_i/\psi_j) & \phi_i < \psi_j \\ [2\phi_i^2/(\phi_i^2 - \psi_j^2)\psi_j] E(\psi_j/\phi_i) - (2/\psi_j) K(\psi_j/\phi_i) & \phi_i > \psi_j \end{cases}, \\
 m_4(\varepsilon_j, \eta_i) &= \begin{cases} (2/\varepsilon_j)K(\eta_i/\varepsilon_j) + [2\varepsilon_j/(\eta_i^2 - \varepsilon_j^2)] E(\eta_i/\varepsilon_j) & \eta_i < \varepsilon_j \\ [2\eta_i/(\eta_i^2 - \varepsilon_j^2)] E(\varepsilon_j/\eta_i) & \eta_i > \varepsilon_j \end{cases}, \tag{35a,b}
 \end{aligned}$$

$$\phi_i, \eta_i = \cos [(i - 1)\pi/(n - 1)], \quad (i = 1, \dots, n)$$

$$\psi_j, \varepsilon_j = \cos [(2j - 1)\pi/(2n - 2)], \quad (j = 1, \dots, n - 1) \tag{36a,b}$$

$$C_1 = C_n = 1/(2n - 2), \quad C_i = 1/(n - 1). \quad (i = 2, \dots, n - 1) \tag{37}$$

Note here that Eqs. (32a) and (32c) are automatically satisfied since $\overline{\overline{F}}_1(\phi)$ and $\overline{\overline{F}}_3(\eta)$ are even functions. The system of equations, Eq. (34), contains $3n/2$ equations for $3n/2$ unknowns, $\overline{\overline{F}}_j(\phi_i)$, ($i = 1, \dots, n/2$; $j = 1 - 3$). However, if n is chosen to be an even integer, it can be shown that Eq. (34b), corresponding to $\psi_{n/2} = 0$, is satisfied automatically since

$$\tau_{rz}(0, L) = 0. \tag{38}$$

The missing equation, Eq. (34b), for $j = n/2$, is complemented by Eq. (32b), which can be converted to

$$\sum_{i=1}^{n/2} C_i \phi_i F_3(\phi_i) = 0. \tag{39}$$

It must be noted here that calculation of the coefficients for $j = n/2$, which corresponds to $r = 0$ in

Eqs. (34a) and (34c) requires special attention. Infinite integrals for kernels $N_{ij}(r, t)$, ($i, j = 1 - 3$) are calculated numerically by using the Laguerre integration formula (Abramowitz and Stegun, 1965).

Numerical Results

The system of linear algebraic equations for the particular problems defined in the previous section is solved and the values of unknown functions $\overline{\overline{F}}_j(\phi_i)$, ($i = 1, \dots, n/2$; $j = 1 - 3$) can be calculated at discrete collocation points. Then, stress distributions, stress intensity factors at the edges of the crack, and the inclusion for an infinite cylinder can be calculated numerically. From the viewpoint of fracture, of particular importance are the stress intensity factors. Stresses become infinitely large at the edges of the crack and the inclusion. In this case,

stress states around those edges can be expressed in terms of the power of stress singularity and stress intensity factors. The normal (Mode I) and the shear (Mode II) components of the stress intensity factors, k_{1a} and k_{2a} , at the edge of the crack may be defined as

$$k_{1a} = \lim_{r \rightarrow a} [2(r - a)]^{1/2} \sigma_z(r, L),$$

$$k_{2a} = \lim_{r \rightarrow a} [2(r - a)]^{1/2} \tau_{rz}(r, L). \quad (40a,b)$$

From Eqs. (20b) and (20c), one may write the expressions for the stress components appearing in Eq. (40), separate the singular parts, calculate the integrals by the method given in Muskhelishvili (1953), substitute in Eq. (40), and obtain

$$k_{1a} = \frac{\kappa}{(\kappa + 1)} p_0 \sqrt{a} \overline{\overline{F}}_1(1) \quad (42)$$

from which

$$\overline{k}_{1a} = \frac{k_{1a}}{p_0 \sqrt{a}} = \frac{\kappa}{(\kappa + 1)} \overline{\overline{F}}_1(1) \quad (43)$$

is obtained for the normalized Mode I stress intensity factor at the edge of the penny-shaped crack. One can similarly write

$$\overline{k}_{2a} = \frac{\kappa}{(\kappa + 1)} \overline{\overline{F}}_2(1) \quad (44)$$

for the normalized Mode II stress intensity factor at the edge of the penny-shaped crack.

Mode II stress intensity factor k_{2b} at the edge of the rigid inclusion may be defined as

$$k_{2b} = \lim_{r \rightarrow b} [2(b - r)]^{1/2} \tau_{rz}(r, 0), \quad (45)$$

and can be calculated in the form

$$k_{2b} = \frac{\sqrt{b}}{2} p_0 \overline{\overline{F}}_3(1). \quad (46)$$

Then, the normalized stress intensity factor becomes

$$\overline{k}_{2b} = \frac{k_{2b}}{p_0 \sqrt{b}} = \frac{\overline{\overline{F}}_3(1)}{2}. \quad (47)$$

For the sake of generalizing the use of the numerical results, dimensionless geometrical parameters a/A , b/A , and L/A normalized by the radius of the cylinder are used. Since the normalized stress intensity

factors are calculated, particular numerical values are not selected for μ and p_0 , and ν is used to describe the material. Some of the calculated results for the following 5 cases are shown in Figures 3-15.

1. Two parallel penny-shaped cracks in an infinite solid:

Figure 3 shows the normalized Mode I and Mode II stress intensity factors \overline{k}_{1a} and \overline{k}_{2a} at the edges of 2 parallel penny-shaped cracks in an infinite solid defined by Eqs. (42) and (43). These figures are produced for the purpose of comparison with the results given by Isida et al. (1985). \overline{k}_{1a} increases and \overline{k}_{2a} decreases with increasing L/a ratio, and remains unchanged after $L/a \cong 4$. As L/a goes to infinity, \overline{k}_{1a} goes to $2/\pi$ and \overline{k}_{2a} goes to zero, which are the values for a single penny-shaped crack. The results seem to be in very good agreement with those given by Isida et al. (1985).

2. Infinite cylinder with a central rigid inclusion:

Figure 4 shows the normalized Mode II stress intensity factor \overline{k}_{2b} at the edge of the rigid inclusion defined by Eq. (46). As can be seen from this figure, \overline{k}_{2b} is negative and it increases with increasing ν , but decreases with increasing b/A ratio. Note that \overline{k}_{2b} is zero when $\nu = 0$. For this situation, there is no Poisson's effect. Consequently, the constraint due to the rigid inclusion disappears and the shearing stresses induced by the inclusion vanish. For $b/A = 1$, the problem reduces to that of a semi-infinite cylinder with a fixed end at $z = 0$ (Gupta, 1974; Kaman and Geçit, 2006). In this special case, the power of singularity γ is < 0.5 and the stress intensity factor calculated on the basis of $\gamma = 0.5$ must tend to zero as $b/A \rightarrow 1$. On the other hand, when $b/A \rightarrow 0$, the problem reduces to that of a finite rigid penny-shaped inclusion in an infinite medium.

3. Infinite cylinder with a single crack:

Figure 5 shows the normalized Mode I stress intensity factor \overline{k}_{1a} at the edge of a single transverse penny-shaped crack in an infinite cylinder, together with the results given in Benthem and Koiter (1973), Leung and Su (1998), and Tsang et al. (2003) for comparison. The results seem to agree with the previous ones, the best agreement being with Benthem and Koiter (1973). The limiting value of \overline{k}_{1a} for $a/A \rightarrow 0$ is $2/\pi$, which is the value for an infinite medium, and it increases with increasing crack radius.

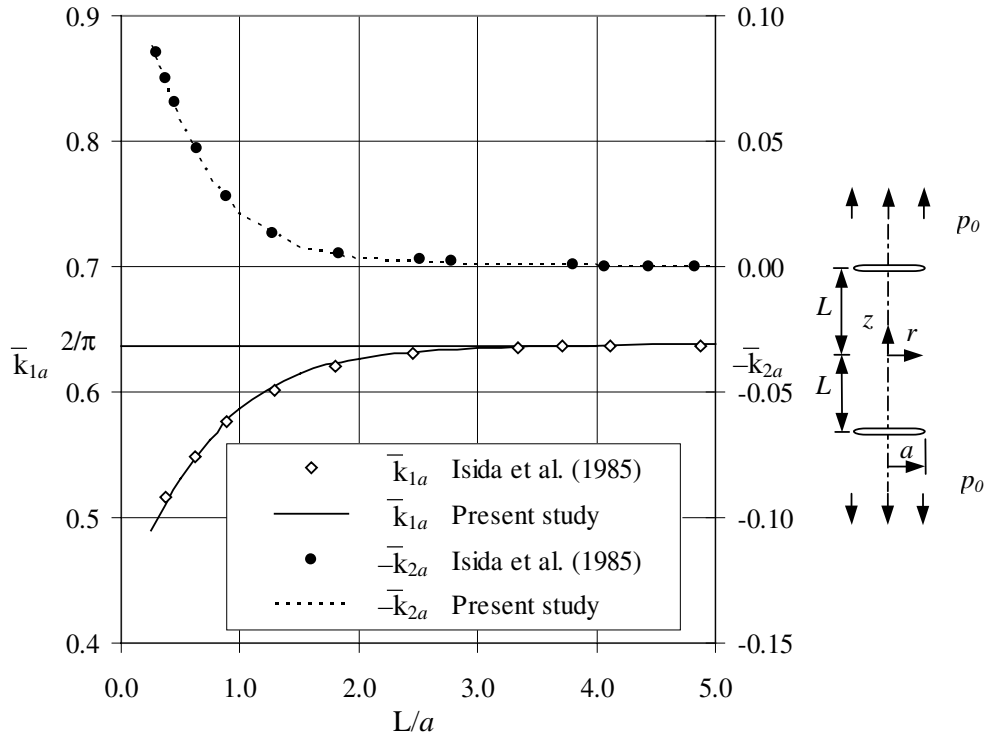


Figure 3. Normalized Mode I \bar{k}_{1a} and Mode II \bar{k}_{2a} stress intensity factors at the edge of 2 parallel penny-shaped cracks in an infinite solid.

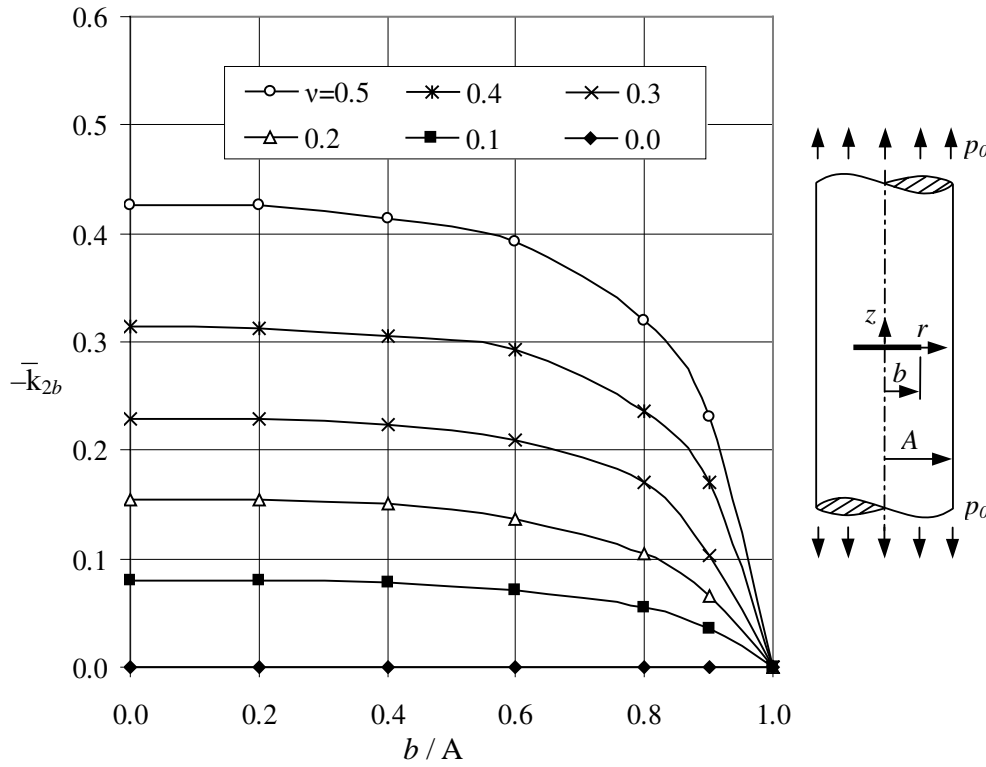


Figure 4. Normalized Mode II stress intensity factor \bar{k}_{2b} at the inclusion edge.

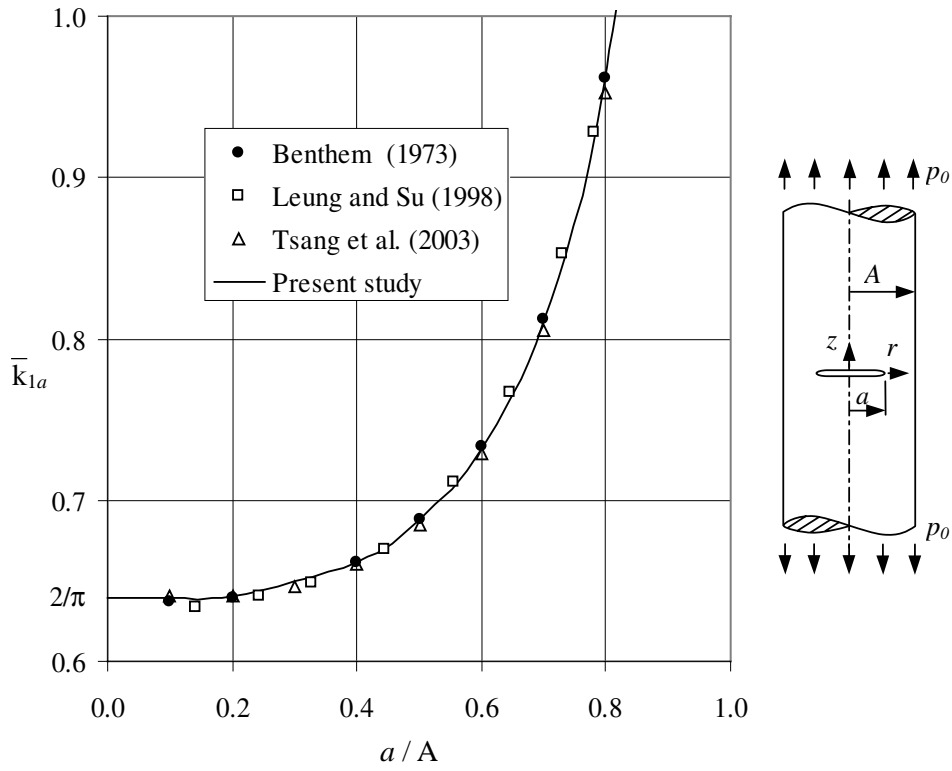


Figure 5. Normalized Mode I stress intensity factor \bar{k}_{1a} at the edge of a single crack, when $\nu = 0.3$.

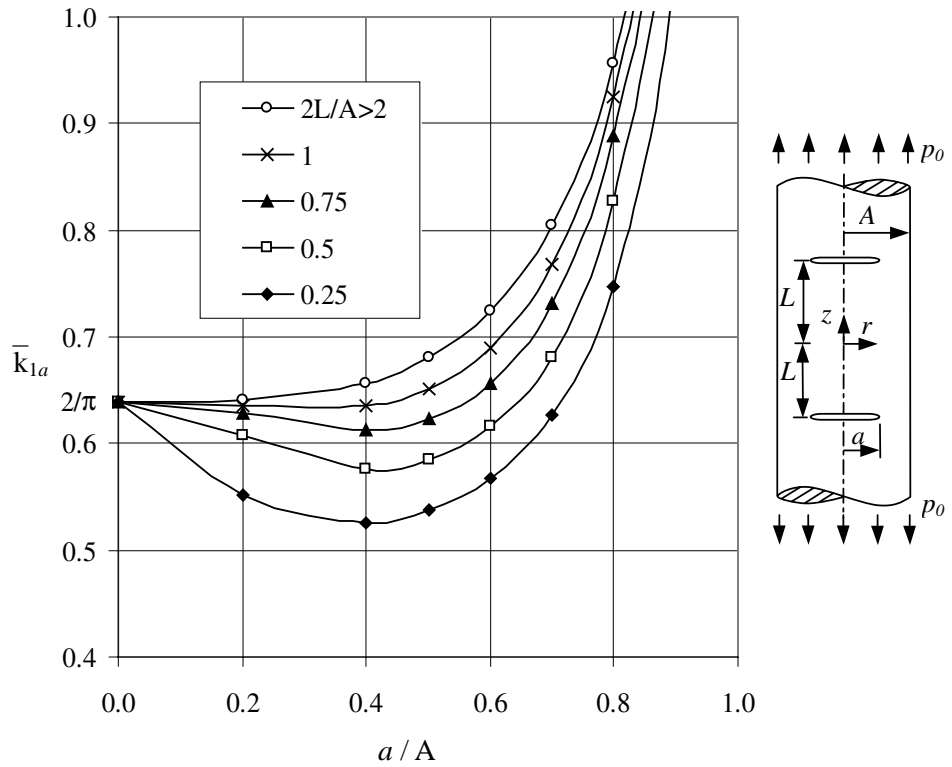


Figure 6. Normalized Mode I stress intensity factor \bar{k}_{1a} at the crack edge, when $\nu = 0.3$.

4. Infinite cylinder with 2 parallel cracks:

Figure 6 shows \bar{k}_{1a} at the edges of 2 parallel penny-shaped cracks in an infinite cylinder. \bar{k}_{1a} is almost insensitive to ν . In most cases, \bar{k}_{1a} increases with increasing a/A and/or L/A ratios. As $L/A \rightarrow \infty$, the infinite cylinder problem with 2 penny-shaped cracks becomes similar to that of an infinite cylinder with a central crack at the $z = 0$ plane. Note that \bar{k}_{1a} converges to $2/\pi$ as $a/A \rightarrow 0$ for fixed values of L/A .

Figure 7 shows variation in \bar{k}_{2a} at the edges of 2 parallel penny-shaped cracks in an infinite cylinder for $\nu = 0.3$. From this figure, one may conclude that \bar{k}_{2a} increases with increasing crack radius. \bar{k}_{2a} decreases as the cracks move away from each other. Note also that \bar{k}_{2a} converges to zero as $a/A \rightarrow 0$ for fixed values of L/A .

In most fracture analyses, approaches based on energy considerations are used with some variation (Geçit, 1988). A crack is claimed to propagate if the rate of release of the stored energy per unit growth of the crack exceeds the rate of change of the surface

energy required by the new surfaces. The energy release rate for the crack may be calculated in the form (Erdogan and Sih, 1963; Geçit, 1988),

$$\frac{\partial \bar{U}}{\partial a} = \frac{\pi^2 a}{\mu} (k_{1a}^2 + k_{2a}^2) \quad (48)$$

where \bar{U} is the strain energy. Figure 8 shows the dimensionless energy release rate

$$\bar{w} = \frac{\mu}{\pi^2 a^2 p_0^2} \frac{\partial \bar{U}}{\partial a} \quad (49)$$

for one crack when $\nu = 0.3$. Note that \bar{w} is larger for larger L/A ratios, i.e. when interaction between the 2 cracks is less. \bar{w} starts with the value $4/\pi^2$, which is the value for a single penny-shaped crack in an infinite medium:

$$k_{1a} = \frac{2}{\pi} p_0 \sqrt{a}, \quad k_{2a} = 0; \quad \bar{w} = \frac{4}{\pi^2} \quad (50)$$

for $a/A \rightarrow 0$ and increases significantly with increasing a/A ratio.

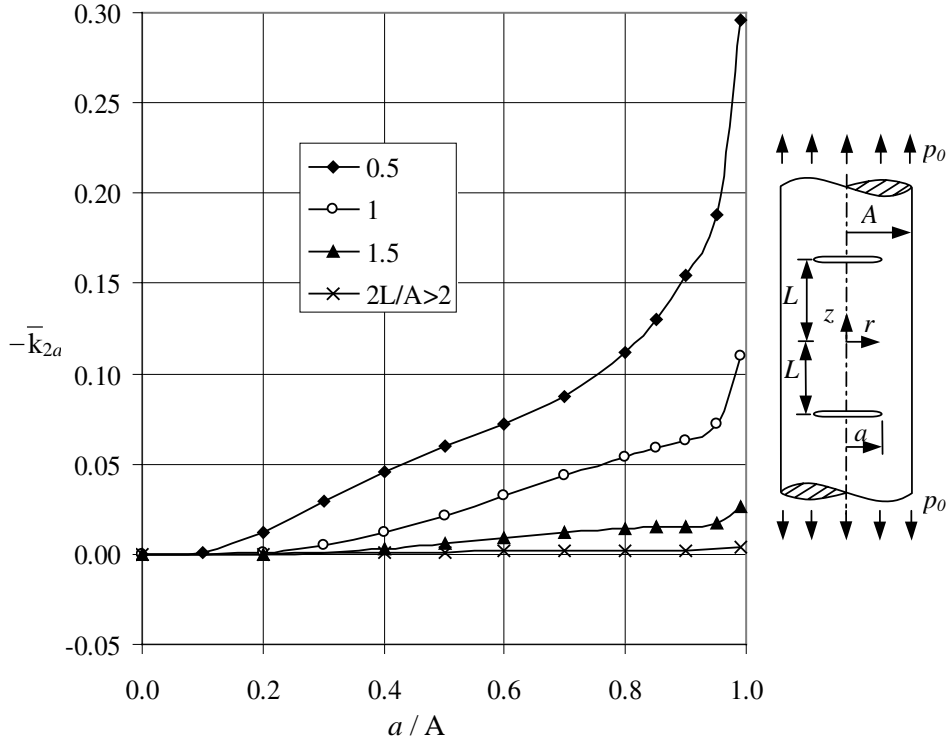


Figure 7. Normalized Mode II stress intensity factor \bar{k}_{2a} at the crack edge, when $\nu = 0.3$.

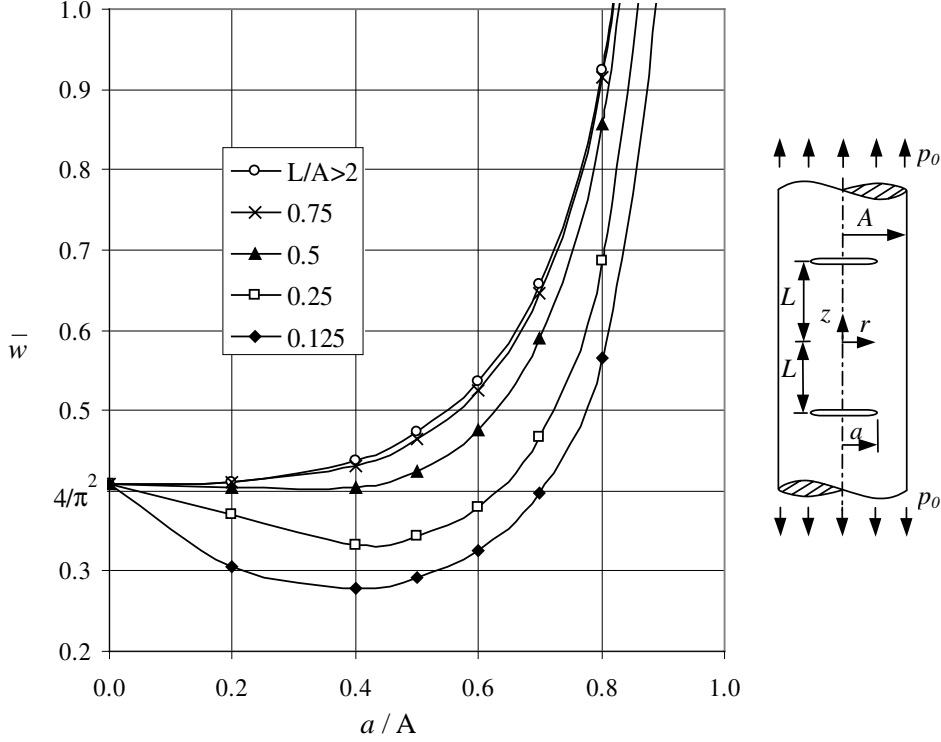


Figure 8. Normalized energy release rate \bar{w} , when $\nu = 0.3$.

If the material of the cylinder is brittle, crack propagation may be expected to take place, as suggested by Erdogan and Sih (1963), in a direction perpendicular to the maximum cleavage stress, which is defined by

$$k_{2a} [1 - 3 \cos(\theta)] - k_{1a} \sin(\theta) = 0,$$

$$3k_{2a} \sin(\theta) - k_{1a} \cos(\theta) < 0. \quad (51a,b)$$

Figure 9 shows the variation in the probable cleavage angle θ at the edge of the penny-shaped crack at the $z = L$ plane, when $\nu = 0.3$. As can be seen in this figure, the 2 cracks propagate away from each other, a tendency that is more pronounced when the cracks are closer to each other. As $a/A \rightarrow 0$, $\theta \rightarrow 0$ for all fixed values of L/A since very small cracks may be thought of as if they are far from all surrounding effects and proceed within their planes.

5. Infinite cylinder with a central rigid inclusion and 2 parallel cracks:

Variation in the normalized Mode I stress intensity factor \bar{k}_{1a} at the edges of penny-shaped cracks with a/A is shown in Figure 10, when $b = 0.5A$. It

seems that \bar{k}_{1a} assumes its minimum value around $a = 0.5A$. This effect is most pronounced for larger values of ν and smaller values of L/A . Relatively high stresses around the edge of the rigid inclusion are responsible for this behavior. It is obvious that the interaction between the rigid inclusion and the cracks is greater when the cracks are closer to the inclusion. The effect of the inclusion is greater for larger ν . In addition to the interaction, \bar{k}_{1a} increases as the crack radius increases. Figure 11 shows variation in \bar{k}_{1a} with b/A , when $a = 0.5A$. Maximum values of \bar{k}_{1a} are realized at $b \cong 0.8A$ for $a = L = 0.5A$.

Figures 12 and 13 show variation in the normalized Mode II stress intensity factor \bar{k}_{2a} at the edges of the cracks. In Figure 12, variation in \bar{k}_{2a} with a/A , when $b = 0.5A$ is given. k_{2a} converges to zero as $a/A \rightarrow 0$ for fixed values of L/A is negative, and its magnitude increases as the crack radius a and/or crack distance L increase(s) for $b = 0.5A$ and $\nu = 0.3$. In Figure 13, variation in \bar{k}_{2a} with b/A is shown for a constant crack radius $a = 0.5A$ and $L = 0.5A$ for several values of ν . As can be seen in Figure 13, \bar{k}_{2a} is always negative. Relatively small variation for smaller values of ν and considerable variation for larger values of ν are observed.

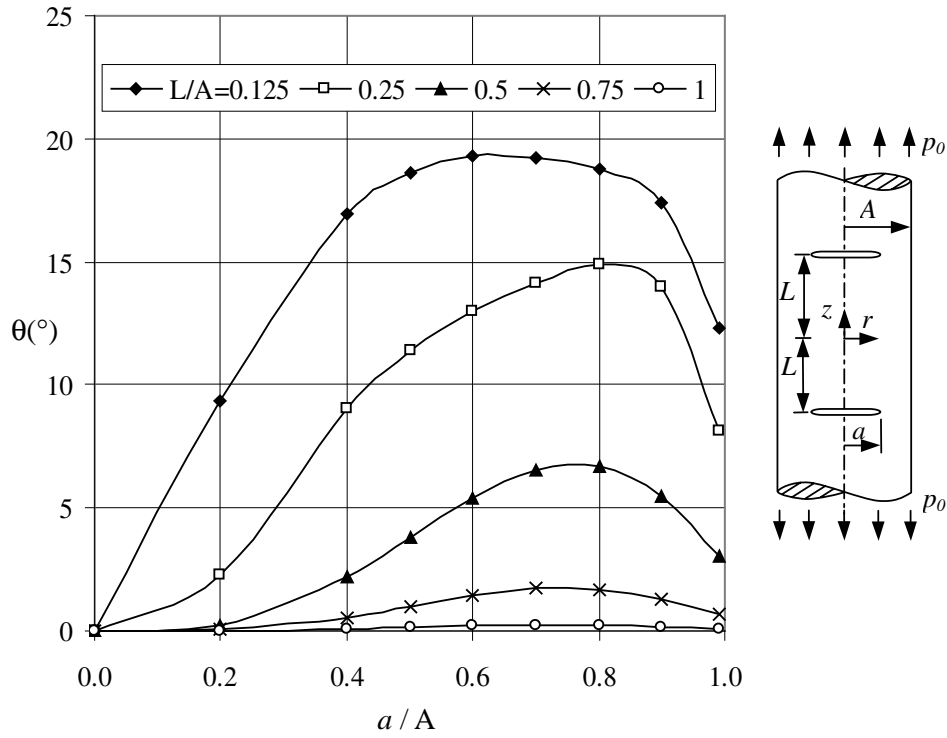


Figure 9. Probable crack propagation angle θ , when $\nu = 0.3$.

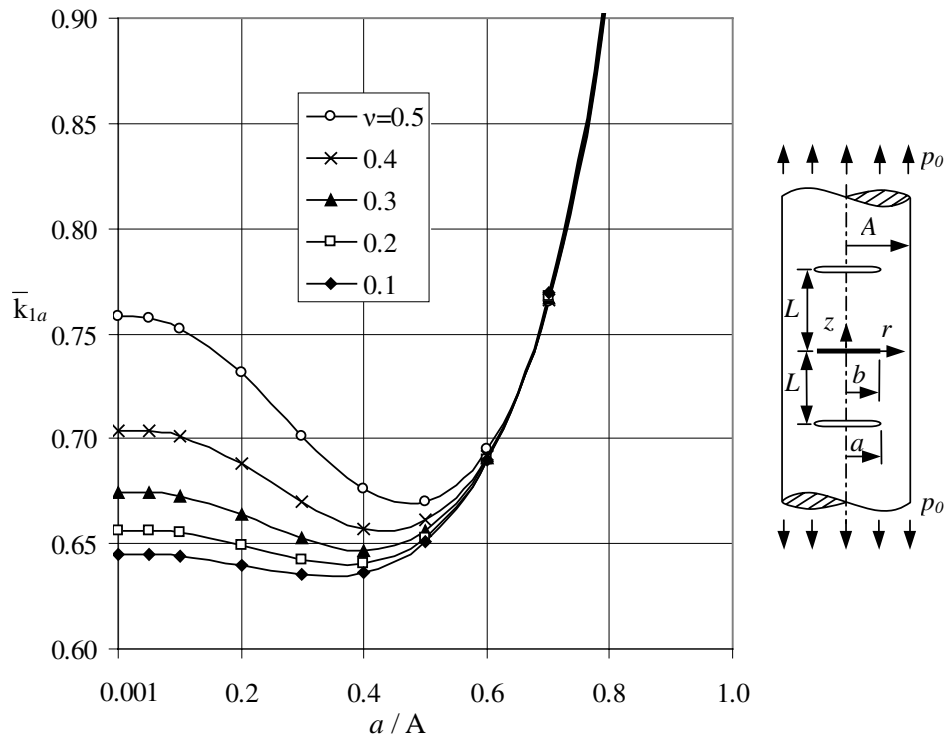


Figure 10. Normalized Mode I stress intensity factor \bar{k}_{1a} , when $b = L = 0.5A$.

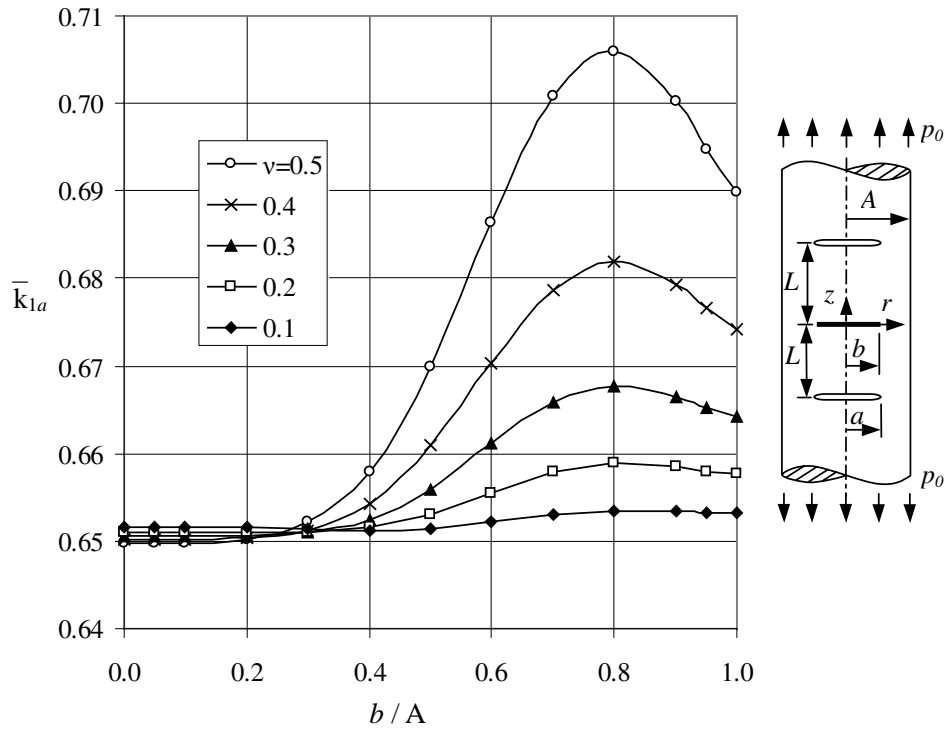


Figure 11. Normalized Mode I stress intensity factor \bar{k}_{1a} , when $a = L = 0.5A$.

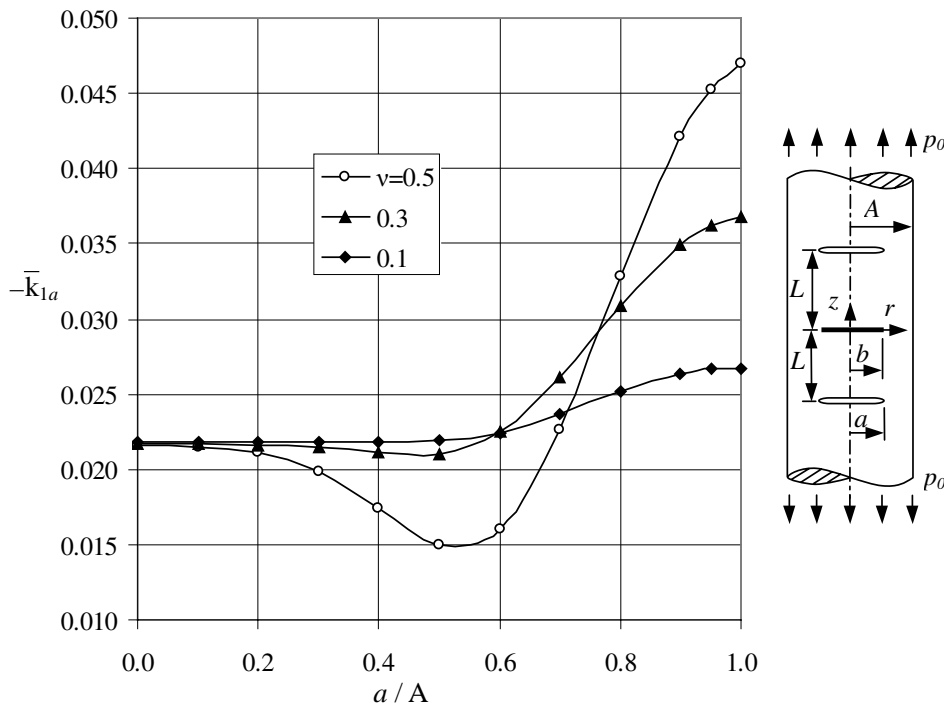


Figure 12. Normalized Mode II stress intensity factor \bar{k}_{2a} , when $b = 0.5A$ and $\nu = 0.3$.

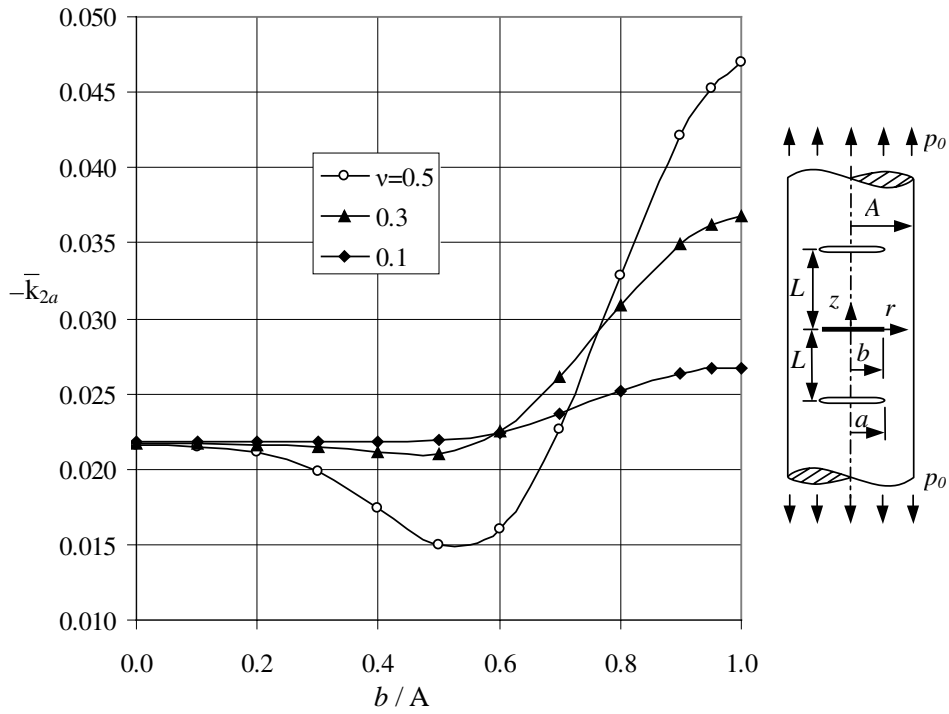


Figure 13. Normalized Mode II stress intensity factor \bar{k}_{2a} , when $a = L = 0.5A$.

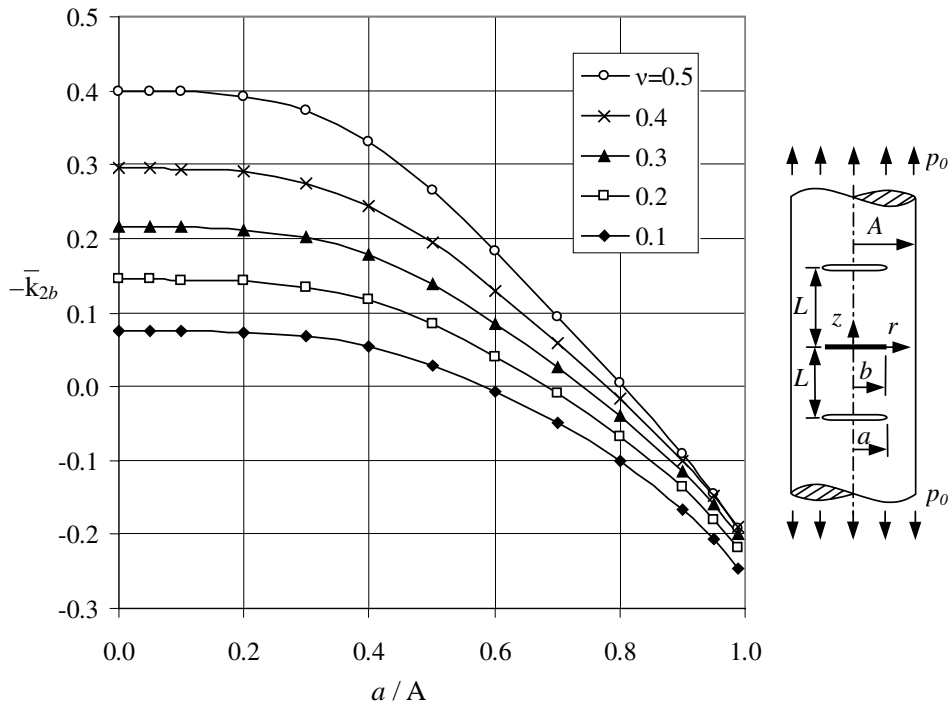


Figure 14. Normalized Mode II stress intensity factor \bar{k}_{2b} , when $b = L = 0.5A$.

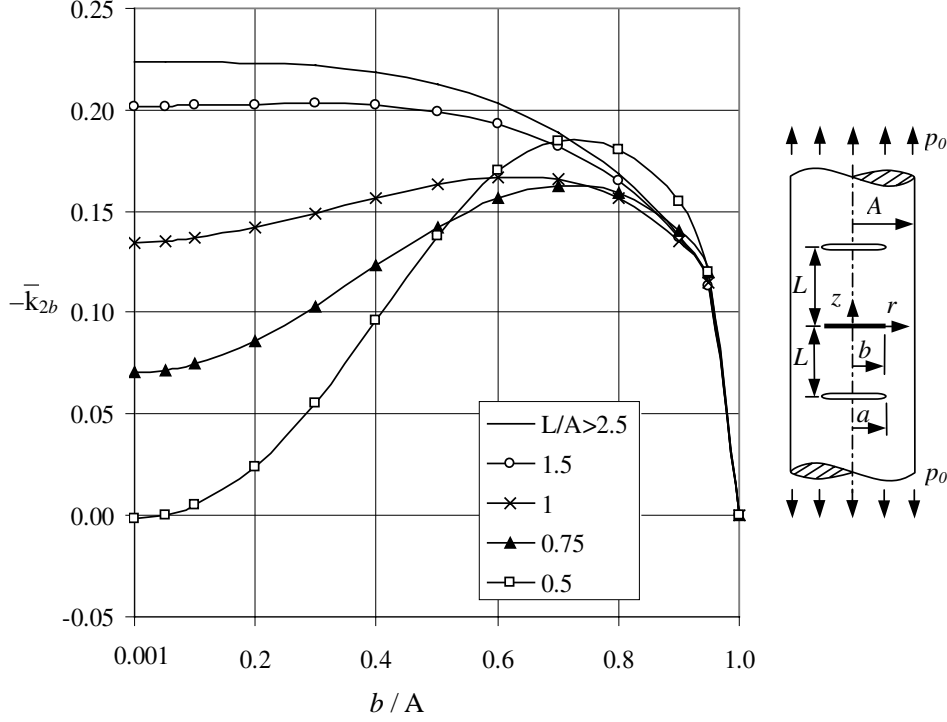


Figure 15. Normalized Mode II stress intensity factor \bar{k}_{2b} , when $a = 0.5A$ and $\nu = 0.3$.

In Figure 14, variation in \bar{k}_{2b} with a/A is shown, when $b = L = 0.5A$. It is observed that \bar{k}_{2b} changes sign from negative to positive as a/A increases. For very small values of a/A , the numerical values given in Figure 4 for $b = 0.5A$ are recovered. Figure 15 shows variation in \bar{k}_{2b} with b/A , when $a = 0.5A$ and $\nu = 0.3$. As can be seen in this figure, \bar{k}_{2b} increases as b/A increases until $b \cong 0.75A$; then it starts decreasing with further increases in b/A for relatively small values of L/A , $L/A < \sim 1$. For greater values of L/A , \bar{k}_{2b} decreases monotonically as b/A increases. For $b/A = 1$, the problem reduces to that of a semi-infinite cylinder with a fixed end at $z = 0$, containing a penny-shaped crack at $z = L$ (Kaman and Geçit, 2006). In this special case, the power of singularity γ is > 0.5 and the stress intensity factor calculated on the basis of $\gamma = 0.5$ must tend to zero as $b/A \rightarrow 1$.

Conclusions

From the formulation and the presented figures, the following conclusions may be deduced:

1. Singularity at the edge of an internal crack or an internal rigid inclusion is $1/2$.
2. The Mode II stress intensity factor \bar{k}_{2b} at the

edge of an internal rigid inclusion in an infinite cylinder is negative and it increases with increasing ν .

3. Mode I and Mode II stress intensity factors \bar{k}_{1a} and \bar{k}_{2a} at the edges of 2 parallel penny-shaped cracks in an infinite cylinder are insensitive to ν (except when $a \rightarrow A$), but they increase as a/A increases and/or L/A decreases.
4. There is considerable interaction between the cracks and the rigid inclusion when ν is large and the cracks are close to the rigid inclusion.

Nomenclature

a	radius of penny-shaped cracks
A	radius of cylinder
b	radius of penny-shaped inclusion
c_i	arbitrary integration constants
C_i	weighting constants of the Gauss-Lobatto polynomials
$f_1(r), f_2(r)$	crack surface displacement derivatives
$f_3(r)$	shear stress jump on rigid inclusion
$f_i^*(t)$	Hölder-continuous functions on cracks and inclusion
$F_i(\alpha)$	Hankel transforms of $f_i(r)$

\overline{F}_i	normalized Hölder-continuous functions on cracks and inclusion	m_i, M_i, R_i, S_i	kernels
$\overline{\overline{F}}_i$	normalized bounded functions on cracks and inclusion	N_{ij}	kernels of the integral equations
$I_0, I_1; K_0, K_1$	modified Bessel functions of the first and second kinds of order zero and one	p_0	intensity of the axial tensile load
J_0, J_1	Bessel functions of the first kind of order zero and one	r, z	radial and axial cylindrical coordinates
k_{1a}, k_{2a}	Mode I and II stress intensity factors at the edge of crack	t	integration variable
k_{1b}, k_{2b}	Mode I and II stress intensity factors at the edge of inclusion	u, w	displacement components in r- and z-directions
$\overline{k}_{1a}, \overline{k}_{2a}$	normalized Mode I and II stress intensity factors at the edge of crack	\overline{U}	strain energy
$\overline{k}_{1b}, \overline{k}_{2b}$	normalized Mode I and II stress intensity factors at the edge of inclusion	\overline{w}	normalized energy release rate
K, E	complete elliptic integrals of the first and the second kinds	α	Fourier and Hankel transform variable
K_{ij}	integrands of the kernels N_{ij}	β, γ	powers of singularity at the edge of cracks and inclusion
L	distance between cracks and inclusion	$\eta, \varepsilon; \phi, \psi$	normalized variables on inclusion and cracks
$m(r, t), m^*(r, t)$	kernels	θ	probable crack propagation angle
		κ	$3 - 4\nu$
		μ	shear modulus of elasticity
		ν	Poisson's ratio
		σ, τ	normal and shearing stresses

References

- Abramowitz, M. and Stegun, I.A., Handbook of Mathematical Functions, Dover Publications, New York, 1965.
- Agarwal, Y.K., "Axisymmetric Solution of the End Problem for a Semi-Infinite Elastic Circular Cylinder and Its Application to Joined Dissimilar Cylinders under Uniform Tension", International Journal of Engineering Science, 16, 985-998, 1978.
- Artem, H.S.A. and Geçit, M.R., "An Elastic Hollow Cylinder under Axial Tension Containing a Crack and Two Rigid Inclusions of Ring Shape", Computers and Structures, 80, 2277-2287, 2002.
- Benthem, J.P. and Minderhoud, P., "The Problem of the Solid Cylinder Compressed between Rough Rigid Stamps", International Journal of Solids and Structures, 8, 1027-1042, 1972.
- Benthem, J.P. and Koiter, W.T., "Asymptotic Approximations to Crack Problems", Mechanics of Fracture 1, Methods of Analysis and Solutions of Crack Problems, (ed. Sih, G.C.), Noordhoff International Publishing, Leyden, The Netherlands, 1973.
- Chaudhuri, R.A., "Three Dimensional Asymptotic Stress Field in the Vicinity of the Circumference of a Penny Shaped Discontinuity", International Journal of Solids and Structures, 40, 3787-3805, 2003.
- Chen, Y.Z., "Stress Intensity Factors in a Finite Length Cylinder with a Circumferential Crack", International Journal of Pressure Vessels and Piping, 77, 439-444, 2000.
- Cook, T.S. and Erdogan, F., "Stresses in Bonded Materials with a Crack Perpendicular to the Interface", International Journal of Engineering Science, 10, 677-697, 1972.
- Erdogan, F. and Sih, G.C., "On the Crack Extension in Plates under Plane Loading and Transverse Shear", Journal of Basic Engineering-Transactions of the ASME, 85, 519-527, 1963.
- Erdol, R. and Erdogan, F., "Thick-Walled Cylinder with an Axisymmetric Internal or Edge Crack", Journal of Applied Mechanics-Transactions of the ASME, 45, 281-286, 1978.
- Geçit, M.R., "Axisymmetric Contact Problem for a Semi-Infinite Cylinder and a Half Space", International Journal of Engineering Science, 24, 1245-1256, 1986.
- Geçit, M.R., "Axisymmetric Pull-off Test for a Cracked Adhesive Layer", Journal of Adhesion Science and Technology, 2, 349-362, 1988.

Gupta, G.D., “An Integral Approach to the Semi-Infinite Strip Problem”, *Journal of Applied Mechanics*, Transactions of the ASME, 40, 948-954, 1973.

Gupta, G.D., “The Analysis of Semi-Infinite Cylinder Problem”, *International Journal of Solids and Structures*, 10, 137-148, 1974.

Isida, M., Hirota, K., Noguchi, H. and Yoshida, T., “Two Parallel Elliptical Cracks in an Infinite Solid Subjected to Tension”, *International Journal of Fracture*, 27, 31-48, 1985.

Kaman, M.O., *Cracked Semi-Infinite Cylinder and Finite Cylinder Problems*, PhD Dissertation, Ankara, Turkey: Department of Engineering Sciences, Middle East Technical University, 2006.

Kaman, M.O. and Geçit, M.R., “Cracked Semi-Infinite Cylinder and Finite Cylinder Problems”, *International Journal of Engineering Science*, 44, 1534-1555, 2006.

Krenk, S., “Quadrature Formulae of Closed Type for Solution of Singular Integral Equations”, *Journal of the Institute of Mathematics and Its Applications*, 22, 99-107, 1978.

Lee, D.S., “Penny-Shaped Crack in a Long Circular Cylinder Subjected to a Uniform Shearing Stress”, *European Journal of Mechanics A-Solids*, 20, 227-239, 2001.

Lee, D.S., “A Long Circular Cylinder with a Circumferential Edge Crack Subjected to a Uniform Shearing Stress”, *International Journal of Solids and Structures*, 39, 2613-2628, 2002.

Leung, A.Y.T. and Su, R.K.L., “Two Level Finite Element Study of Axisymmetric Cracks”, *International Journal of Fracture*, 89, 193-203, 1998.

Meshii, T. and Watanabe, K., “Stress Intensity Factor for a Circumferential Crack in a Finite-Length Thin to Thick-Walled Cylinder under an Arbitrary

Biquadratic Stress Distribution on the Crack Surface”, *Engineering Fracture Mechanics*, 68, 975-986, 2001.

Muskhelishvili, N.I., *Singular Integral Equations*, P. Noordhoff, Gröningen, Holland, 1953.

Nied, H.F. and Erdogan, F., “The Elasticity Problem for a Thick-Walled Cylinder Containing a Circumferential Crack”, *International Journal of Fracture*, 22, 277-301, 1983.

Selvadurai, A.P.S., “Mechanics of a Rigid Circular Disk Bonded to a Cracked Elastic Half-Space”, *International Journal of Solids and Structures*, 39, 6035-6053, 2002.

Sneddon, I.N. and Welch, J.T., “A Note on the Distribution of Stress in a Cylinder Containing a Penny-Shaped Crack”, *International Journal of Engineering Science*, 1, 411-419, 1963.

Toygur, E.M. and Geçit, M.R., “Cracked Infinite Cylinder with Two Rigid Inclusions under Axisymmetric Tension”, *International Journal of Solids and Structures*, 43, 4777-4794, 2006.

Tsang, D.K.L., Oyadiji, S.O. and Leung, A.Y.T., “Multiple Penny-Shaped Cracks Interaction in a Finite Body and Their Effect on Stress Intensity Factor”, *Engineering Fracture Mechanics*, 70, 2199-2214, 2003.

Xiao, Z.M., Lim, M.K. and Liew, K.M., “Determination of Stress Field in an Elastic Solid Weakened by Parallel Penny-Shaped Cracks”, *Acta Mechanica*, 114, 83-94, 1996.

Yetmez, M. and Geçit, M.R., “Finite Strip with a Central Crack under Tension”, *International Journal of Engineering Science*, 43, 472-493, 2005.

Williams, M.L., “Stress Singularities Resulting from Various Boundary Conditions in Angular Corners of Plates in Extension”, *Journal of Applied Mechanics*, 19, 526-528, 1952.

Appendix

The expressions for the integrands $K_{ij}(r, t, \alpha)$ ($i, j = 1 - 3$) appearing in Eq. (25) are as follows

$$K_{11}(r, t, \alpha) = \frac{2\alpha}{d_0} [t\alpha g_7 H_{00} + (2g_5 - g_1)H_{01} - 2tr\alpha^2 H_{10} + r\alpha g_5 H_{11}] c_L^2, \quad (\text{A.1})$$

$$K_{12}(r, t, \alpha) = \frac{2}{Ad_0} [A\alpha g_1(2g_4 - 1)H_{00} + A\alpha^2 g_7 H_{01} + A\alpha^2 g_5 H_{10} - 2Atr\alpha^3 H_{11} \\ + (\kappa_1 + 2g_3)A\alpha R_0 - \kappa_1 A_1(r\alpha R_1 + 2R_0)] c_L s_L, \quad (\text{A.2})$$

$$K_{13}(r, t, \alpha) = -\frac{\alpha}{2d_0} [2t\alpha g_7 H_{00} + g_9 H_{01} - 4tr\alpha^2 H_{10} + 2r\alpha g_6 H_{11}] c_L, \quad (\text{A.3})$$

$$K_{21}(r, t, \alpha) = \frac{2\alpha}{d_0} [-2tr\alpha^2 H_{00} + r\alpha g_5 H_{01} + t\alpha g_5 H_{10} - g_1 H_{11}] c_L s_L, \quad (\text{A.4})$$

$$K_{22}(r, t, \alpha) = \frac{2\alpha}{Ad_0} [Ar\alpha g_5 H_{00} - 2Atr\alpha^2 H_{01} - Ag_1 H_{10} + At\alpha g_5 H_{11} + \kappa_1 (AA_0 R_1 - rA_1 R_0)] s_L^2, \quad (\text{A.5})$$

$$K_{23}(r, t, \alpha) = \frac{\alpha}{2d_0} [4tr\alpha^2 H_{00} - 2r\alpha g_6 H_{01} - 2t\alpha g_5 H_{10} + g_8 H_{11}] s_L, \quad (\text{A.6})$$

$$K_{31}(r, t, \alpha) = \frac{1}{d_0} [-2t\alpha^2 g_6 H_{00} + \alpha g_8 H_{01} + 2t\alpha g_2 T_0 - g_2 g_5 T_1] c_L, \quad (\text{A.7})$$

$$K_{32}(r, t, \alpha) = -\frac{1}{A\alpha d_0} [-A\alpha^2 g_1 (2 + \kappa_1 g_4) H_{00} + 2At\alpha^3 (g_1 + g_3 + \kappa_1 g_4) H_{01} + A\alpha g_2 g_5 T_0 - 2At\alpha^2 g_2 T_1 - \kappa_1 g_2 A_1 + \kappa_1^2 \alpha R_0 A_1 + A\alpha^2 (2\kappa_1 - g_3) R_0 A_0] s_L, \quad (\text{A.8})$$

$$K_{33}(r, t, \alpha) = \frac{1}{2d_0} \{2t\alpha^2 g_6 H_{00} - [g_1 + 2\kappa_1 (\kappa + g_3 + g_5)] H_{01} - 2t\alpha g_2 T_0 + g_2 g_6 T_1\}, \quad (\text{A.9})$$

where

$$\kappa_1 = \kappa + 1, \quad \kappa_2 = (\kappa - 1)^2, \quad \kappa_3 = \kappa - 3, \quad c_L = \cos(\alpha L), \quad s_L = \sin(\alpha L), \quad (\text{A.10})$$

$$g_1 = \kappa_1 + 2A^2\alpha^2, \quad g_2 = 4\alpha R_0 + 2r\alpha^2 R_1, \quad g_3 = 2A^2\alpha^2 A_0 K_0, \quad g_4 = A_1 K_1, \quad g_5 = g_3 + g_1 g_4,$$

$$g_6 = g_5 + \kappa_1, \quad g_7 = g_5 - 4, \quad g_8 = 2g_1 + \kappa_1 g_5, \quad g_9 = 2g_1 - \kappa_3 g_3 + \kappa_2 g_1 g_4, \quad (\text{A.11})$$

$$H_{ij} = R_i T_j, \quad (j = 0, 1), \quad R_i = I_i(r\alpha), \quad T_i = I_i(t\alpha), \quad A_i = I_i(A\alpha), \quad K_i = K_i(A\alpha), \quad (i = 0, 1) \quad (\text{A.12})$$